


## ORIGINAL ARTICLE

**Mucosal-associated invariant T cells correlate with myocardial ischaemia and remodelling in coronary artery disease**Jiafu Wang<sup>1,a</sup>, Song Li<sup>2,a</sup>, Xianling Zhou<sup>2,a</sup>, Hongxing Wu<sup>1</sup>, Xiaolan Ouyang<sup>1</sup>, Zhuoshan Huang<sup>1</sup>, Long Peng<sup>1</sup>, Qian Chen<sup>3</sup>, Yuman Wu<sup>2</sup>, Zhitong Li<sup>4,5</sup>, Ziyi Peng<sup>4,5</sup>, Yi Yang<sup>6</sup>, Yan Lu<sup>4,5</sup>, Xixiang Tang<sup>7</sup>, Yue Li<sup>4,5</sup> & Suhua Li<sup>1</sup> 

1 Department of Cardiovascular Medicine, The Third Affiliated Hospital of Sun Yat-sen University, Guangzhou, China

2 Department of Clinical Immunology, The Third Affiliated Hospital of Sun Yat-sen University, Guangzhou, China

3 School of Biomedical Sciences, The Chinese University of Hong Kong, Hong Kong, China

4 Guangdong Provincial Key Laboratory of Allergy &amp; Clinical Immunology, Guangzhou Medical University, Guangzhou, China

5 The Second Affiliated Hospital, Guangzhou Medical University, Guangzhou, China

6 Department of Endocrinology and Metabolic Diseases, The Third Affiliated Hospital of Sun Yat-sen University, Guangzhou, China

7 VIP Medical Service Center, The Third Affiliated Hospital of Sun Yat-sen University, Guangzhou, China

**Correspondence**

Y Lu and Y Li, Guangdong Provincial Key Laboratory of Allergy &amp; Clinical Immunology, Guangzhou Medical University, Guangzhou, China.

E-mail: [luyan@gzhmu.edu.cn](mailto:luyan@gzhmu.edu.cn);[liyue@gzhmu.edu.cn](mailto:liyue@gzhmu.edu.cn)

X Tang, VIP Medical Service Center, The Third Affiliated Hospital of Sun Yat-sen University, Guangzhou, China.

E-mail: [tangxx3@mail.sysu.edu.cn](mailto:tangxx3@mail.sysu.edu.cn)

S Li, Department of Cardiovascular Medicine, The Third Affiliated Hospital of Sun Yat-sen University, Guangzhou, China.

E-mail: [lisuhua3@mail.sysu.edu.cn](mailto:lisuhua3@mail.sysu.edu.cn)<sup>a</sup>Equal contributors.

Received 16 September 2024;

Revised 27 January and 14 March 2025;

Accepted 14 March 2025

doi: 10.1002/cti.70029

*Clinical & Translational Immunology*

2025; 14: e70029

**Abstract**

**Objectives.** Myocardial ischaemia and remodelling are major contributors to the progression and mortality of coronary artery disease (CAD). Previous studies have shown immune cell alterations in CAD patients, but their characteristics and associations with myocardial ischaemia and remodelling remain unclear. **Methods.** We compared immune cell changes among patients without CAD, those with CAD and those with CAD and heart failure (HF). **Results.** We found a progressive reduction in circulating mucosal-associated invariant T (MAIT) cells across the three patient groups. MAIT cells exhibited increased expression of activation markers (CD69 and PD-1) and cytotoxic molecules (such as granzyme B). The features of MAIT cells were correlated positively with worsening clinical indicators of myocardial ischaemia and remodelling, including the Gensini score, cTnI, NT-proBNP, LVEF and E/e'. Additionally, the reduction, activation and cytotoxicity of MAIT cells were associated with indicators of myocardial fibrosis (sST2, Gal-3, PICP and PIIINP), a central pathological mechanism of myocardial remodelling. Finally, we preliminarily explored potential triggers for MAIT cell abnormalities in CAD patients and found that impaired intestinal barrier function and increased circulating bacterial antigens may contribute to these changes. **Conclusions.** During CAD progression, we observed a decrease in circulating MAIT cells. Enhanced activation and cytotoxicity of MAIT cells are associated with myocardial ischaemia and remodelling in CAD patients with heart failure, potentially triggered by gut microbial leakage. Our findings suggest a novel strategy for monitoring and intervention in disease progression.

**Keywords:** coronary artery disease, gut barrier permeability, heart failure, MAIT cells, myocardial fibrosis

## INTRODUCTION

Coronary artery disease (CAD) affects approximately 126.5 million people worldwide, leading to 10.6 million new cases and 8.9 million deaths annually.<sup>1</sup> During CAD progression, atherosclerosis of the coronary arteries can lead to a reduction in myocardial blood flow and oxygen supply. As the coronary arteries narrow and atherosclerotic plaques accumulate, these changes can lead to myocardial remodelling, characterised by cardiac dysfunction and myocardial fibrosis, ultimately weakening the myocardium and culminating in heart failure (HF).<sup>2,3</sup> Therefore, myocardial ischaemia and remodelling are major contributors to the progression and mortality of CAD. Despite available treatments including anti-thrombotic therapy, statins and 'quadruple therapy' for HF, many patients with CAD still experience the progression of myocardial ischaemia and remodelling. Therefore, identifying new targets for disease monitoring and intervention is of significant clinical importance.

Over the last two decades, emerging evidence from both clinical and experimental studies has shown that CAD is a chronic inflammatory disease, in which the immune system plays a prominent role in its development and progression.<sup>4,5</sup> All stages of atherosclerosis, from the accumulation of atherogenic lipoproteins in the arterial wall to plaque formation and rupture, involve a complex interplay of innate and adaptive immune responses, which regulate the inflammatory and anti-inflammatory actions of immune cells such as macrophages<sup>6,7</sup> and lymphocytes.<sup>8,9</sup> Clinical trials have shown that targeting inflammation leads to a decreased incidence of CAD.<sup>10–12</sup> Meanwhile, it has also been found that the most beneficial effects of statins are because of the reduction in vascular inflammation, to some extent, independent of their lipid-lowering function.<sup>13,14</sup> Although the inflammatory biology of CAD has been translated into therapeutic strategies, the specificity of current inflammatory biomarkers is low, and they inadequately reflect the actual biological processes, since the precise mechanisms of the inflammatory pathway, especially the initiation factors, are still not fully defined.

Therefore, studying immune alterations during CAD progression and identifying specific immune cell types that associate with the progression of myocardial ischaemia and remodelling in patients with CAD not only helps understand the mechanism of inflammatory initiation but also represents a potent therapeutic strategy.

In recent years, a distinctive unconventional T-cell subset known as 'mucosal-associated invariant T (MAIT) cells' has garnered increasing interest from immunologists and clinicians. MAIT cells represent one of the most abundant subsets of T cells in humans, participating in various infectious and non-infectious diseases, with remarkable sensitivity to inflammatory responses. MAIT cells exhibit a transcriptional profile marked by the expression of promyelocytic leukaemia zinc finger (PLZF) and retinoic acid-related orphan receptor  $\gamma$ t (ROR $\gamma$ t).<sup>15</sup> They also express eomesodermin (Eomes) and T box transcription factor 21 (TBX21 or T-bet), which are differentially expressed in effector and memory CD8<sup>+</sup> T cells and play a critical role in T-cell activation.<sup>15</sup> In response to antigen and cytokine stimulation, MAIT cells can maintain high expression levels of granzyme B and perforin.<sup>16</sup> It is worth noting that CD8<sup>+</sup> T cells possessing this cytotoxic function have been demonstrated to play a pivotal role in the development and progression of human CAD.<sup>17</sup> This suggests a potential role of MAIT cells in the context of CAD. Previous studies have found that MAIT cells are activated in metabolic disorders, which are important risk factors for CAD.<sup>18,19</sup> Furthermore, it has been established that MAIT cells actively participate in the progression of fibrosis in multiple organs, including the kidney, liver and lung.<sup>20–22</sup> Fibrosis is a key mechanism in cardiac remodelling that ultimately leads to HF in CAD. Moreover, the activation of MAIT cells is associated with dysbiosis in the gut microbiota,<sup>23</sup> with recent studies underscoring the significant role of gut microbiota dysregulation in CAD and HF.<sup>24,25</sup> All these intriguing observations prompted us to hypothesise that in the context of persistent inflammation in CAD patients, alterations in the characteristics and functions of MAIT cells may occur and contribute to CAD progression.

To examine this hypothesis in the human context, peripheral blood samples were collected from a cohort of participants, including 48 non-CAD participants (without CAD or HF), 75 CAD individuals (without HF) and 47 CAD+HF individuals (with both CAD and HF). We initiated the study by analysing the characteristic alterations in inflammation and MAIT cell profiles within the context of the diseases, seeking their potential associations with myocardial ischaemia and remodelling in patients with CAD. Furthermore, we conducted a preliminary investigation into the potential role of bacterial antigens derived from a compromised gut barrier in patients with CAD as drivers of MAIT cell alterations. In summary, our findings indicate that the peripheral reduction, activation and cytotoxicity of MAIT cells are associated with myocardial ischaemia and adverse remodelling in patients with CAD. Impaired gut barrier function and increased bacterial antigens may potentially act as triggering factors. These discoveries may serve as potential targets for predicting and intervening in myocardial ischaemia and remodelling in patients with CAD.

## RESULTS

### Baseline characteristics of patients

Table 1 summarises the baseline characteristics of the study cohort. Participants in the CAD group exhibited a greater number of well-established risk factors associated with CAD, including advanced age ( $P < 0.001$ ), elevated homocysteine levels ( $P < 0.05$ ) and elevated blood glucose levels ( $P < 0.001$ ), than subjects in the non-CAD group. As disease severity increased, patients with CAD+HF were older and had higher levels of HbA1c, homocysteine, serum creatinine and uric acid, as well as elevated N-terminal pro-B-type natriuretic peptide (NT-proBNP) levels, compared with the non-CAD and CAD groups (all  $P < 0.05$ ). Additionally, CAD patients displayed a higher red cell distribution width standard deviation ( $P < 0.001$ ), lactate dehydrogenase ( $P < 0.01$ ) and gamma-glutamyl transpeptidase ( $P < 0.05$ ), all of which have been associated with systemic chronic inflammation, with further increases observed in patients with CAD+HF. However, no significant differences in gender, body mass index (BMI), systolic blood pressure (SBP), diastolic blood pressure (DBP) or lipid profile were observed among the groups.

### Association of systemic inflammation coincides with CAD and HF

To assess immune cell and inflammatory changes in CAD and HF, we examined changes in immune markers using routine clinical blood tests and analysed several indices indicative of continuous systemic inflammation. Compared with the non-CAD group, CAD and CAD+HF patients exhibited significantly elevated absolute counts of white blood cells (WBC) and neutrophils, along with increased C-reactive protein (CRP) levels (Figure 1a–c). The neutrophil-to-lymphocyte ratio (NLR) reflects the inflammatory state, characterised by an increased neutrophil count and a reduced lymphocyte count, and has been shown to independently predict the occurrence and progression of stable atherosclerosis.<sup>26</sup> NLR significantly increased in CAD patients and increased further in the CAD+HF group (Figure 1d). The Systemic Immune-Inflammation Index (SII) and the Systemic Inflammatory Response Index (SIRI) are comprehensive indices used to assess systemic inflammation and immune response. These indices consider neutrophil and lymphocyte counts in the blood, along with either platelet or monocyte counts. Both indices are employed in the analysis of inflammation and disease relevance in CAD.<sup>27</sup> Significant increases in SII and SIRI were observed in CAD patients, with SII showing further elevation in the CAD+HF group (Figure 1e and f). The Acute Inflammatory Stress Index (AISI) is a recently developed inflammatory marker used to reflect the inflammatory status in acute illnesses or stress.<sup>28</sup> AISI exhibited significant elevation in both CAD and CAD+HF patients (Figure 1g). These findings suggest that CAD is associated with a systemic inflammatory state, which becomes more pronounced in the presence of HF complications. Notably, subjects with CAD+HF also displayed a trend of decreased lymphocyte count (Figure 1h), a marker of systemic inflammation closely associated with adverse outcomes in CAD and HF.<sup>29</sup>

Collectively, our analysis of clinical test data from the enrolled study population revealed pronounced elevations in WBC, neutrophil and CRP levels in both CAD and CAD+HF patients. Additionally, several inflammatory markers were elevated. These findings indicate the presence of a systemic inflammatory state in these patients. Further analysis is required to investigate changes

**Table 1.** Clinical characteristics of patients

Variables	Non-CAD (n = 48)	CAD (n = 75)	CAD + HF (n = 47)	P-value
Age, years	57.5 (48, 63.25)	64 (57, 71.5) <sup>&amp;&amp;</sup>	73 (60, 83) <sup>&amp;&amp;##</sup>	< 0.001*
Male, %	20 (41.70)	47 (62.70)	28 (59.60)	0.061
BMI, kg (m <sup>2</sup> ) <sup>-1</sup>	24.02 ± 3.16	24.33 ± 2.82	24.01 ± 3.27	0.801
Hypertension	25 (52.10)	53 (70.70)	36 (76.60)	0.027*
SBP, mmHg	129.46 ± 18.97	130.49 ± 21.87	133.15 ± 21.42	0.672
DBP, mmHg	85.29 ± 14.00	80.88 ± 12.79	79.70 ± 12.67	0.086
RDW-SD, fL	41.58 ± 3.22	43.05 ± 3.94 <sup>&amp;</sup>	46.31 ± 6.23 <sup>&amp;&amp;##</sup>	< 0.001*
HGB, g L <sup>-1</sup>	135.47 ± 16.70	136.23 ± 15.35	127.72 ± 23.74	0.57
PLT, ×10 <sup>9</sup> L <sup>-1</sup>	227.02 ± 57.08	213.64 ± 57.66	210.53 ± 67.98	0.389
TC, mmol L <sup>-1</sup>	4.32 ± 0.86	4.32 ± 1.55	4.40 ± 1.46	0.95
TG, mmol L <sup>-1</sup>	1.32 (0.97, 1.80)	1.09 (0.76, 1.79)	1.2 (0.94, 1.63)	0.303
LDL-C, mmol L <sup>-1</sup>	2.48 ± 0.77	2.67 ± 1.27	2.69 ± 1.29	0.48
HDL-C, mmol L <sup>-1</sup>	1.19 ± 0.51	0.99 ± 0.23	1.02 ± 0.38	0.063
ApoA-I, mg L <sup>-1</sup>	1.29 (1.11, 1.42)	1.22 (1.09, 1.38)	1.36 (1.16, 1.49)	0.054
ApoB100, mg L <sup>-1</sup>	0.89 (0.65, 1.12)	0.85 (0.62, 1.07)	0.81 (0.76, 0.96)	0.621
Lp(a), mg L <sup>-1</sup>	175 (103.25, 362.50)	248.50 (149.75, 337.00)	170.00 (96.00, 343.00)	0.332
HCY, µmol L <sup>-1</sup>	10.65 ± 2.46	12.66 ± 4.36 <sup>&amp;</sup>	15.09 ± 5.24 <sup>&amp;&amp;##</sup>	< 0.001*
UA, µmol L <sup>-1</sup>	334.58 ± 93.43	357.81 ± 89.17	416.50 ± 115.76 <sup>&amp;&amp;##</sup>	< 0.001*
SCr, µmol L <sup>-1</sup>	64.89 ± 4.03	68.92 ± 7.00	94.25 ± 25.33 <sup>&amp;&amp;##</sup>	< 0.001*
LDH, U L <sup>-1</sup>	168.75 ± 31.82	183.27 ± 35.57	199.09 ± 36.16 <sup>&amp;&amp;##</sup>	0.002*
ALP, U L <sup>-1</sup>	66.38 (53.25, 75.25)	70.92 (55.00, 79.00)	79.09 (59.00, 82.00)	0.473
γ-GT, U L <sup>-1</sup>	20.00 (16.00, 27.80)	26.00 (20.00, 44.00) <sup>&amp;&amp;</sup>	26.00 (18.00, 56.00)	0.028*
FPG, mmol L <sup>-1</sup>	5.11 ± 1.13	5.99 ± 1.98	6.55 ± 2.77	< 0.001*
HbA1c, %	5.65 ± 1.00	6.60 ± 1.46 <sup>&amp;&amp;</sup>	6.58 ± 1.63 <sup>&amp;&amp;</sup>	< 0.001*
FIB, g L <sup>-1</sup>	3.25 (2.73, 3.59)	3.19 (2.80, 3.82)	3.53 (3.07, 4.28) <sup>&amp;#</sup>	0.042*
D-dimer, mg L <sup>-1</sup>	0.22 (0.22, 0.44)	0.22 (0.22, 0.36)	0.435 (0.22, 0.68)	0.143
SF, µg L <sup>-1</sup>	214.22 (146.80, 328.10)	264.70 (141.90, 379.00)	188.95 (82.00, 294.10)	0.236
NT-proBNP, pg mL <sup>-1</sup>	70 (70, 141.00)	107 (70, 180.50)	1280 (409, 3955) <sup>&amp;&amp;##</sup>	< 0.001*
Gensini score	1.96 ± 3.16	23.08 ± 23.38 <sup>&amp;&amp;</sup>	22.85 ± 21.80 <sup>&amp;&amp;</sup>	< 0.001*

Normally distributed data are presented as the mean ± standard deviation (SD); non-normally distributed variables are represented as median (interquartile range, IQR), and categorical variables are shown as n (%). <sup>&</sup>P < 0.05 and <sup>&&</sup>P < 0.01 indicates significant differences compared to the non-CAD group; <sup>#</sup>P < 0.05 and <sup>##</sup>P < 0.01 indicates significant differences compared to the CAD group; \*P < 0.05 indicates statistical significance in the overall three-group ANOVA analysis.

ALP, alkaline phosphatase; ApoA-I, apolipoprotein A-I; ApoB100, apolipoprotein B100; BMI, body mass index; DBP, diastolic blood pressure; FBG, fasting blood glucose; HCY, homocysteine; HDL-C, high-density lipoprotein cholesterol; HGB, haemoglobin; LDH, lactate dehydrogenase; LDL-C, low-density lipoprotein cholesterol; Lp(a), lipoprotein(a); NT-proBNP, N-terminal pro-B-type natriuretic peptide; PLT, platelet count; RDW-SD, red cell distribution width standard deviation; SBP, systolic blood pressure; SCr, serum creatinine; SF, serum ferritin; TC, total cholesterol; TG, triglycerides; UA, uric acid; γ-GT, gamma-glutamyl transpeptidase.

in specific immune cell subsets associated with the CAD disease state, aiming to provide a comprehensive understanding of the immune alterations.

### Progressive loss of MAIT cells in CAD and HF

To gain a more in-depth understanding of the changes in immune cell populations within the enrolled cohort, peripheral blood samples were obtained, and peripheral blood mononuclear cells (PBMCs) were extracted. Subsequently, we conducted an

immunophenotypic analysis using flow cytometry, as illustrated in Supplementary figure 2. Notably, T and B cells were slightly reduced in the CAD + HF group (Figure 2a and b), while monocytes remained unchanged across the groups (Figure 2c). To examine which T-cell subsets were specifically altered, we first analysed the frequency of conventional T cells and found no significant differences among the groups (Figure 2d and e). To our surprise, one subset of the unconventional T cells, the MAIT cells, decreased by half in the CAD group and further declined to one-fifth in the CAD + HF group

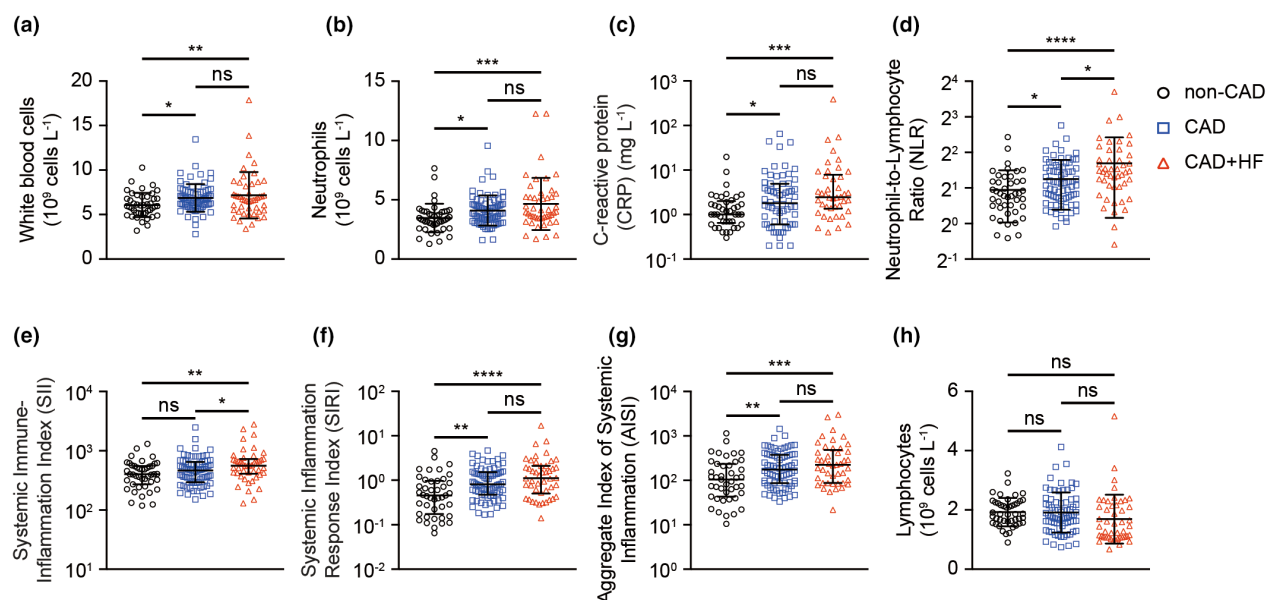


**Figure 1.** Systemic inflammation coincides with CAD. **(a–c)** Changes in circulating WBC **(a)**, neutrophil **(b)** and CRP levels **(c)** among the non-CAD ( $n = 48$ ), CAD ( $n = 75$ ) and CAD + HF ( $n = 47$ ) groups. **(d–g)** Changes in inflammatory indices, including the Neutrophil-to-Lymphocyte Ratio (NLR) **(d)**, Systemic Immune-Inflammation Index (SII) **(e)**, Systemic Inflammation Response Index (SIRI) **(f)** and Aggregate Index of Systemic Inflammation (AISII) **(g)** among the non-CAD ( $n = 48$ ), CAD ( $n = 75$ ) and CAD + HF ( $n = 47$ ) groups. **(h)** Circulating lymphocyte counts among the groups. Each symbol represents an individual sample. Error bars represent mean  $\pm$  SD **(a, b, d, h)** and median with IQR **(c, e–g)**. Statistical significance: ns  $P > 0.05$ ; \*  $P < 0.05$ ; \*\*  $P < 0.01$ ; \*\*\*  $P < 0.001$ ; \*\*\*\*  $P < 0.0001$ . Statistical analysis was conducted using one-way ANOVA or the Kruskal-Wallis H test for comparisons among the three groups, followed by *post hoc* LSD analysis or Dunn's test for pairwise comparisons.

(Figure 2f and g). MAIT cells are a type of innate-like T cell. Other innate-like T cells, such as iNKT and  $\gamma\delta$  T cells, did not show significant changes within the non-CAD, CAD and CAD + HF groups (Figure 2h–k). To further investigate whether the number of MAIT cells changed, we analysed the absolute count of MAIT cells and found that it also decreased (Supplementary figure 3a). We also observed that the non-MAIT cell population (CD161<sup>−</sup> TCR V $\alpha$ 7.2<sup>+</sup>) exhibited variability across different samples. However, upon analysing all the samples collectively, no significant difference was detected (Supplementary figure 3b, c).

Given that age has been reported to influence MAIT cell frequency,<sup>30</sup> and considering that patients in the CAD + HF group were relatively older, we conducted a sub-group analysis by matching age and serum creatinine levels within our cohort. The results revealed that the trend of decreasing MAIT cell frequency during the progression of CAD still persists (Supplementary figure 3d–f). Considering the substantial decrease in the abundance of MAIT cells, we utilised ROC

analysis to evaluate their changes as potential indicators and predictors of the disease. ROC curve analysis demonstrated that the reduction in MAIT cells could serve as a stronger predictor for CAD and CAD + HF than NLR, T and B-cell frequency, with an AUC value of 0.796 for CAD (95% CI: 0.723 ~ 0.869,  $P < 0.001$ ) and 0.756 for CAD + HF (95% CI: 0.672 ~ 0.841,  $P < 0.001$ ) (Figure 2l and m). Overall, we observed a progressively decreasing frequency of MAIT cells in the peripheral blood of patients, from non-CAD to CAD, and further to CAD + HF patients. Moreover, the alterations in MAIT cells are significant and serve as better predictive indicators than NLR, T and B cells, indicating that MAIT cells may play a role in the progression of the disease and could be a potential therapeutic target for intervention.

### Enhanced activation and cytotoxicity of MAIT cells in CAD and HF

To uncover the comprehensive changes in MAIT cells in CAD, we performed an extensive



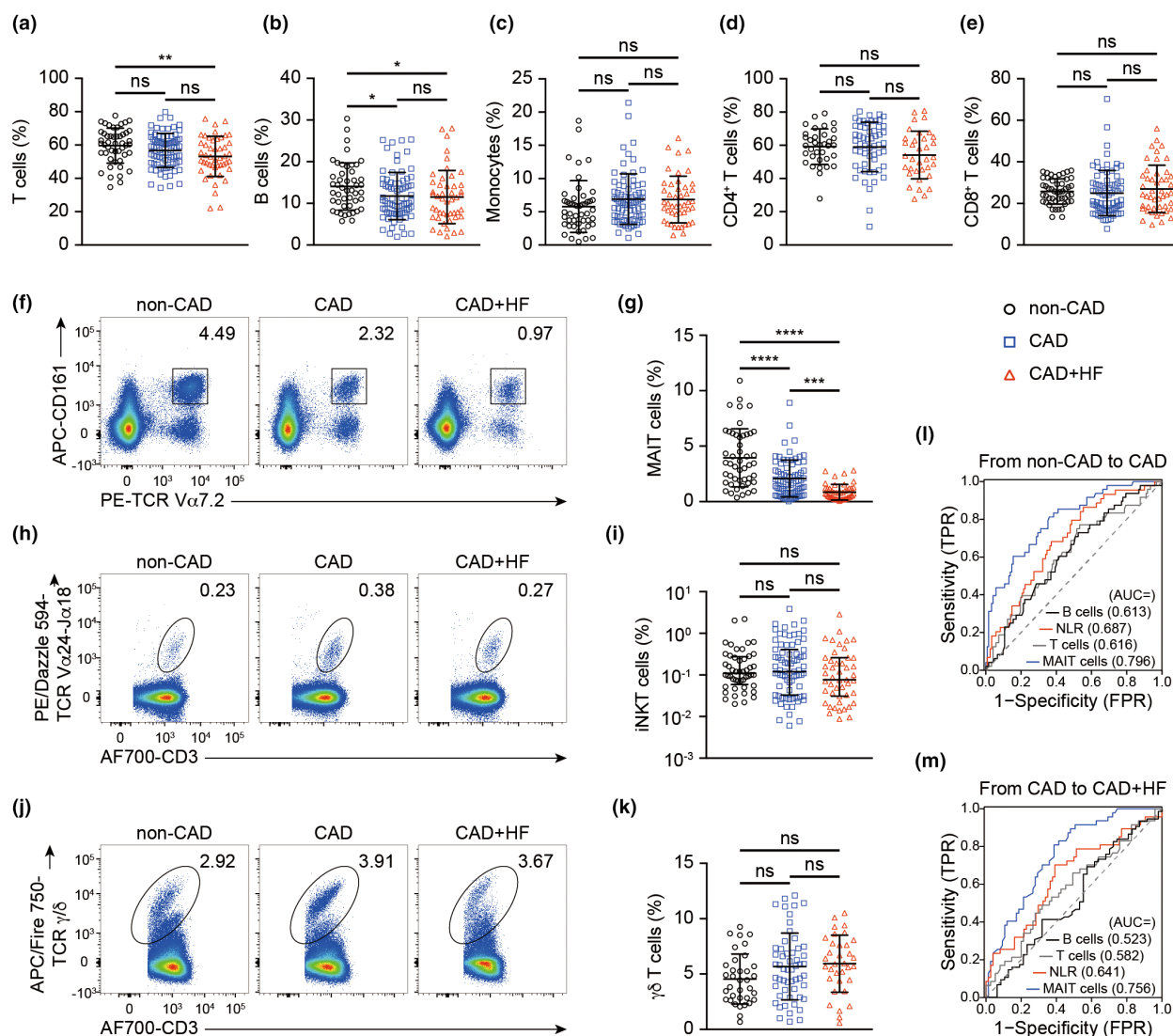


**Figure 2.** Decline in MAIT cell frequency is associated with CAD progression. **(a–c)** Frequency of T cells **(a)**, B cells **(b)** and monocytes **(c)** among CD45<sup>+</sup> cells in the non-CAD ( $n = 48$ ), CAD ( $n = 75$ ) and CAD + HF ( $n = 47$ ) groups. **(d, e)** Frequency of CD4<sup>+</sup> **(d)** and CD8<sup>+</sup> T **(e)** cell subsets among T cells in the three groups. Flow cytometry analysis of MAIT **(f, g)**, iNKT **(h, i)** and  $\gamma\delta$ T cells **(j, k)** among T cells was conducted for each group. Sample sizes for specific analyses were non-CAD ( $n = 48, 48, 32$  for **f, i** and **k**, respectively), CAD ( $n = 75, 75, 47$  for **f, i** and **k**, respectively) and CAD + HF ( $n = 47, 47, 28$  for **g, i** and **k**, respectively). **(l, m)** ROC curve analysis evaluating the diagnostic performance of MAIT cell frequency in distinguishing non-CAD from CAD **(l)** and CAD from CAD + HF **(m)**. Each symbol represents an individual sample **(a–e, g, i, k)**. Error bars represent mean  $\pm$  SD **(a–e, g, k)** and median with IQR **(i)**. Statistical significance: ns  $P > 0.05$ ; \*  $P < 0.05$ ; \*\*  $P < 0.01$ ; \*\*\*  $P < 0.001$ ; \*\*\*\*  $P < 0.0001$ . One-way ANOVA was conducted for comparisons among the three groups, followed by *post hoc* LSD analysis for pairwise comparisons.

analysis of their phenotype and functionality. In the CAD group, there was a slight upregulation of CD69 expression in MAIT cells, which was further enhanced in the CAD + HF group (Figure 3a and b). CD69 is a type II C-type lectin receptor that is rapidly expressed on the cell surface following stimulation. It serves as a well-known activation

marker for MAIT cells and is also considered a hallmark of tissue retention,<sup>22</sup> influencing the migration and acquisition of effector or regulatory phenotypes in T cells.<sup>31</sup> Notably, even when analysed in an age-matched manner, the frequency of CD69<sup>+</sup> MAIT cells was significantly higher in the CAD + HF group (Supplementary

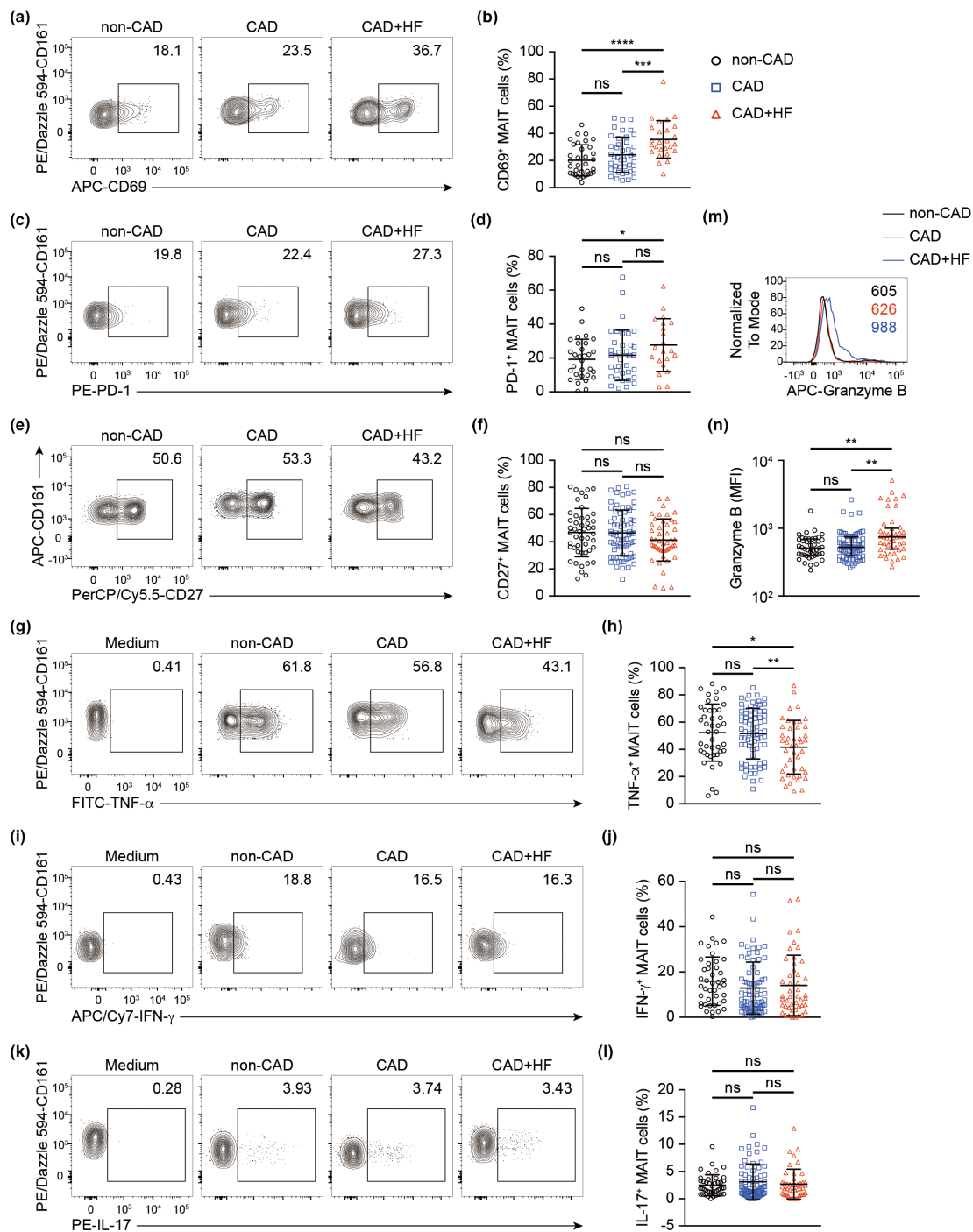


**Figure 3.** MAIT cells display increased activation and cytotoxicity in CAD and HF patients. **(a–f)** Flow cytometry analysis of CD69<sup>+</sup> **(a, b)**, PD-1<sup>+</sup> **(c, d)** and CD27<sup>+</sup> **(e, f)** MAIT cells among total MAIT cells in the non-CAD ( $n = 34$ , 30 and 48, respectively), CAD ( $n = 43$ , 37 and 74, respectively) and CAD + HF ( $n = 26$ , 21 and 47, respectively) groups. **(g–l)** Flow cytometry analysis of TNF- $\alpha$ <sup>+</sup> **(g, h)**, IFN- $\gamma$ <sup>+</sup> **(i, j)** and IL-17<sup>+</sup> **(k, l)** MAIT cells among total MAIT cells following PMA and ionomycin stimulation in the non-CAD ( $n = 43$ ), CAD ( $n = 72$ ) and CAD + HF ( $n = 46$ ) groups, as well as under unstimulated (medium) conditions. **(m, n)** Flow cytometry analysis of granzyme B mean fluorescence intensity (MFI) in MAIT cells from the non-CAD ( $n = 43$ ), CAD ( $n = 72$ ) and CAD + HF ( $n = 46$ ) groups. Each symbol represents an individual sample. Error bars represent mean  $\pm$  SD **(b, d, f, h, j, k)** and median with IQR **(n)**. Statistical significance: ns  $P > 0.05$ ; \*  $P < 0.05$ ; \*\*  $P < 0.01$ ; \*\*\*  $P < 0.001$ ; \*\*\*\*  $P < 0.0001$ . One-way ANOVA or the Kruskal-Wallis H test was conducted for group comparisons, followed by *post hoc* LSD analysis or Dunn's test for pairwise comparisons.

figure 3g). However, the absolute number of CD69<sup>+</sup> MAIT cells progressively decreased because of the reduction in total MAIT cell count (Supplementary figure 3h). In the CAD + HF group, MAIT cells exhibited higher levels of the activation/exhaustion marker PD-1 expression (Figure 3c and d), indicating excessive activation of MAIT cells in patients with CAD and HF. However, we found no significant differences in CD27 expression, a co-stimulatory receptor,<sup>32</sup> among the three groups (Figure 3e and f).

Next, we assessed the functional properties of MAIT cells by examining cytokine production. After stimulating the cells with phorbol 12-myristate 13-acetate (PMA) and ionomycin, MAIT cells from the CAD + HF group showed a reduction in the production of TNF- $\alpha$ , while there were no significant changes in IFN- $\gamma$  and IL-17 (Figure 3g–i). Additionally, MAIT cells from the CAD + HF group demonstrated significant upregulation in granzyme B production (Figure 3m and n), suggesting enhanced cytotoxic capabilities. Resting human MAIT cells typically lack granzyme B expression, an essential cytotoxic granule protein required for effective cytotoxic activity. Upon rapid activation triggered by recognition of bacterial-derived riboflavin metabolites bound to MHC class I-related protein 1 (MR1), MAIT cells upregulate granzyme B expression and can kill homologous target cells.<sup>33</sup> We also tested the levels of granzyme B and TNF- $\alpha$  in plasma and found a significant increase in granzyme B production in CAD + HF patients compared with non-CAD individuals. However, TNF- $\alpha$  levels did not differ significantly among the groups (Supplementary figure 3i, j).

In summary, MAIT cells exhibit increased activation characteristics and enhanced cytotoxic function with increasing severity of CAD. This may contribute to disease progression and warrant further investigation into their correlation.

### **MAIT cell alterations are linked to myocardial ischaemia and remodelling**

The prognosis of CAD patients primarily depends on myocardial ischaemia and remodelling, which affect myocardial blood supply and cardiac function. Given our findings of differences in the abundance, activation and cytokine secretion of MAIT cells in CAD, we further analysed the associations between these features and clinical indicators of myocardial ischaemia and remodelling, including the Gensini

score (Supplementary figure 1), cardiac troponin I (cTnI) and cardiac ultrasound parameters. The Gensini score is a widely used angiographic scoring system for quantifying the severity of CAD. cTnI is a highly sensitive and specific biomarker for myocardial injury, with elevated levels indicating myocardial necrosis. Cardiac ultrasound parameters, such as left ventricular ejection fraction (LVEF) and wall motion abnormalities, provide a non-invasive assessment of cardiac function and are crucial for evaluating the extent of myocardial remodelling. By correlating these clinical indicators with MAIT cell features, we aim to understand the role of MAIT cells in the pathophysiology of myocardial ischaemia and remodelling and explore their potential as biomarkers for disease severity and prognosis.

We found that the reduction, activation and cytotoxicity of MAIT cells significantly correlated with increasing Gensini scores and cTnI levels (Figure 4a–h). This positive correlation between MAIT cell features and Gensini scores indicates that the severity of coronary artery stenosis, as quantified by the Gensini score, is associated with changes in the immune response, specifically the activation and cytotoxicity of MAIT cells. Furthermore, the correlation with cTnI levels, a biomarker of myocardial injury, further suggests that MAIT cell activation is linked to the extent of myocardial damage.

Additionally, the reduction, expression of CD69 and cytotoxicity (granzyme B release) of MAIT cells significantly correlated with worsening NT-proBNP and E/e' levels (Figure 4i–s), which are indicators of cardiac function. This suggests that these immune cells may also be involved in the progression of cardiac remodelling. This is further supported by the partial association with atrial enlargement (LA and RA) and IVS thickening, which are structural changes indicative of advanced cardiac disease (Figure 4j–p).

Together, these results highlight the potential of MAIT cells as biomarkers for the severity and progression of CAD and its associated complications, providing a new perspective for the diagnosis and management of patients with myocardial ischaemia and remodelling.

### **MAIT cell alterations correlate with myocardial fibrosis**

In individuals with CAD, the death of ischemic myocardial cells triggers a multi-stage reparative response that ultimately results in the



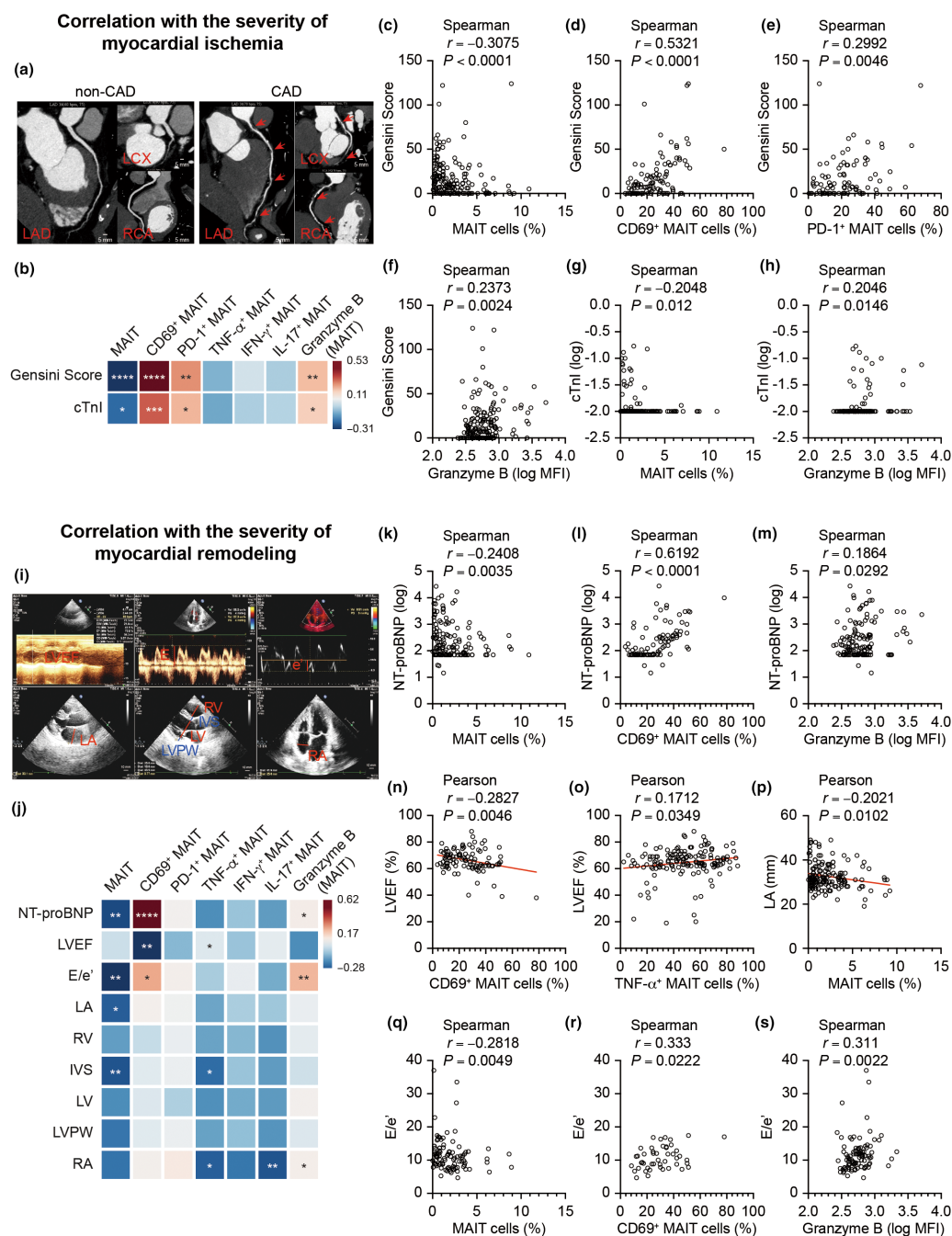


**Figure 4.** Altered MAIT characteristics correlate with the severity of atherosclerosis and HF in CAD patients. **(a)** Curved reconstructions from coronary CT angiography (CTA) illustrating coronary artery narrowing. Arrows indicate the narrowed areas (scale bar = 5 mm). **(b–h)** Double-matrix correlation heatmap **(b)** and correlation plots **(c–h)** depicting the relationship between circulating MAIT cells and severity indicators of atherosclerosis. **(i)** Echocardiographic assessment included three-chamber, two-chamber and apical four-chamber views, the long-axis view of the left ventricle in M-mode, and colour and tissue Doppler imaging. These measurements included atrial and ventricular dimensions (LA, left atrium; LV, left ventricle; RA, right atrium; RV, right ventricle), septal thickness (IVS), posterior wall thickness (LVPW) and cardiac function parameters, including left ventricular ejection fraction (LVEF) for contraction and E/e' for relaxation (scale bar: 10 mm). **(j–s)** Double-matrix correlation heatmap **(j)** and correlation plots **(k–s)** depicting the relationship between circulating MAIT cells and severity indicators of HF. Each symbol represents a single individual. Heatmap colour intensity represents the correlation coefficient ( $r$ ) **(c–h, k–s)**. Statistical significance: ns  $P > 0.05$ ; \*  $P < 0.05$ ; \*\*  $P < 0.01$ ; \*\*\*  $P < 0.001$ ; \*\*\*\*  $P < 0.0001$ . Spearman's correlation test was applied to non-normally distributed data (Gensini score, cTnI, NT-proBNP and E/e'), whereas Pearson correlation analysis was used for normally distributed data (LVEF, LA, RV, IVS, LV, LVPW and RA).

replacement of damaged areas with fibrotic scar tissue. Excessive fibrotic responses are detrimental, as they lead to a gradual deterioration of cardiac function, ultimately resulting in heart failure.<sup>2</sup> Given the challenges of diagnosing myocardial fibrosis through tissue biopsy, several non-invasive biomarkers have been proposed for its assessment.<sup>34</sup> In this study, we measured four highly specific indicators of myocardial fibrosis in the plasma of the enrolled population: (a) Soluble suppression of tumorigenicity-2 (sST2), which acts as an antagonist of the IL-33/ST2-L signalling pathway, promotes fibrosis and adverse remodelling following cardiac injury.<sup>35</sup> (b) Galectin-3 (Gal-3), a member of the  $\beta$ -galactoside-binding protein family, is expressed and secreted by macrophages. It can bind to and activate fibroblasts, leading to collagen deposition in the extracellular matrix and subsequent progressive myocardial fibrosis.<sup>36</sup> (c) The carboxy-terminal propeptide of type I procollagen (PICP), which is formed during the extracellular conversion of type I procollagen into mature type I collagen fibers.<sup>37</sup> (d) The amino-terminal propeptide of type III procollagen (PIIINP), which is a peptide formed during the extracellular conversion of type III procollagen into mature type III collagen fibers.<sup>38</sup>

We observed significant increases in the circulating levels of sST2, Gal-3, PICP and PIIINP in patients with CAD and HF (CAD + HF), indicating the presence of myocardial fibrosis (Figure 5a–d). Next, we analysed the correlations between these four myocardial fibrosis indicators and MAIT cell frequency, activation status, as well as cytokine secretion and cytotoxicity (Figure 5e–o). We found that the frequency of MAIT cells was negatively correlated with sST2 and PIIINP (Figure 5e–g), while the frequency of CD69<sup>+</sup> MAIT cells exhibited positive correlations with Gal-3, PICP and PIIINP (Figure 5e and h–j). Moreover, both PD-1<sup>+</sup> and IFN- $\gamma$ <sup>+</sup> MAIT cell frequencies positively correlated with PICP (Figure 5e, k and l). These data were consistent with previous findings that MAIT cells exhibit an enhanced activation phenotype but decreased frequency in the peripheral blood of CAD and HF patients. Additionally, the secretion of granzyme B in MAIT cells was positively correlated with sST2, Gal-3, and PICP (Figure 5e and m–o). These results suggest that the cytotoxicity of activated MAIT cells may participate in the process of myocardial fibrosis,

thereby increasing the severity of CAD and promoting the occurrence of HF complications.

### Gut barrier dysfunction and bacterial antigen leakage may initiate MAIT cell alterations

Given the observed alterations in MAIT cell activation in CAD and HF patients, we investigated whether there was an increase in stimulatory antigens under those conditions. We first assessed the bacterial load in the blood of the cohort using real-time PCR and found a significant decrease in the cycle threshold (Ct) for bacterial 16S rDNA levels in the blood of the CAD + HF group compared with non-CAD patients (Figure 6a). Additionally, we quantified the bacterial load in the plasma using *Escherichia coli* (*E. coli*) strain DH10B as a reference template and found that the average bacterial counts were significantly higher in the CAD + HF group than in the non-CAD group (Figure 6b).

Next, we sought to identify the sources of the increased bacterial antigens. The human body is colonised by a vast number of microorganisms, with the greatest diversity and abundance found in the intestinal tract.<sup>39</sup> Disruption of the gut microbiota, ecological imbalance and metabolic abnormalities have emerged as important factors influencing immune system composition and cardiac repair in CAD patients.<sup>40</sup> Therefore, we assessed the integrity of the gut barrier by measuring plasma levels of tight junction protein 1 (ZO-1), lipopolysaccharide-binding protein (LBP) (a marker of gut leak) and intestinal fatty acid-binding protein (iFABP) (a marker of intestinal epithelial cell damage). Both ZO-1 and LBP levels were significantly elevated in the CAD and CAD + HF groups (Figure 6c and d), indicating impaired gut barrier integrity in these patients. However, iFABP levels did not show significant differences among the groups (Figure 6e), likely because of its extremely low detectable concentration in circulation (<2 ng mL<sup>-1</sup>) and the limited detection time window (<48 h).<sup>41</sup>

We hypothesised that compromised gut barrier integrity in CAD patients allows intestinal bacteria to leak into the bloodstream, which in turn alters MAIT cell characteristics and contributes to myocardial fibrosis. Correlation analyses supported this hypothesis. Specifically, the concentration of bacteria in plasma was

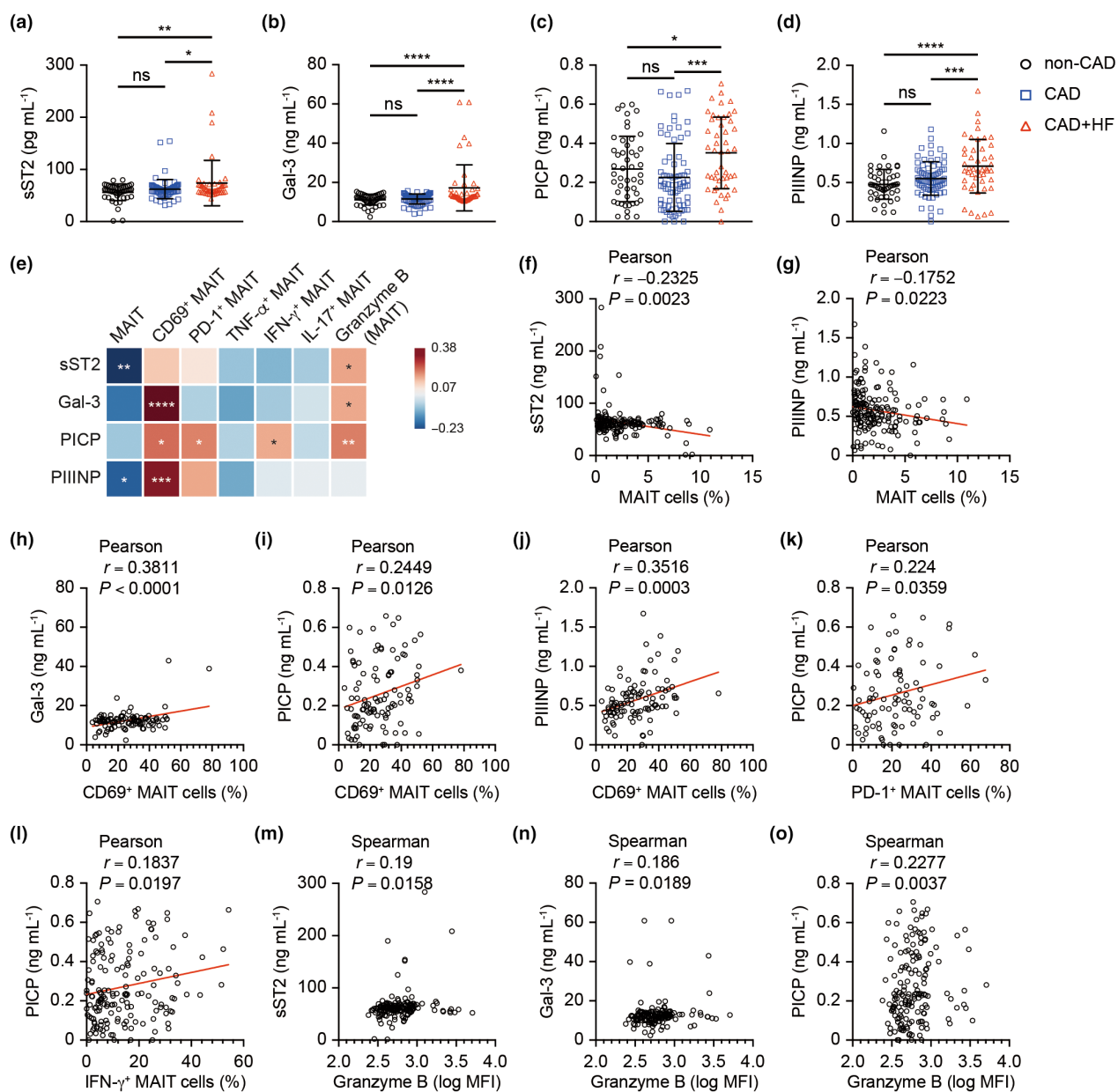


**Figure 5.** Altered MAIT cell characteristics are strongly associated with circulating cardiac fibrosis biomarkers. **(a–d)** ELISA quantification of plasma sST2 **(a)**, Gal-3 **(b)**, PICP **(c)** and PIIINP **(d)** levels in non-CAD ( $n = 48$ ), CAD ( $n = 75$ ) and CAD + HF ( $n = 47$ ) groups. **(e)** Double-matrix correlation heatmap illustrating relationships between MAIT cell features and circulating cardiac fibrosis biomarkers. **(f, g)** Correlations between the frequency of circulating MAIT cells and the levels of plasma sST2 **(f)** and PIIINP **(g)** (data pairs  $n = 170$ ). **(h–j)** Correlations between the frequency of CD69<sup>+</sup> MAIT cells and the levels of plasma Gal-3 **(h)**, PICP **(i)** and PIIINP **(j)** (data pairs  $n = 103$ ). **(k)** Correlations between the frequency of PD-1<sup>+</sup> MAIT cells and the levels of PICP (data pairs  $n = 88$ ). **(l)** Correlations between the frequency of IFN- $\gamma$ <sup>+</sup> MAIT cells and the levels of PICP (data pairs  $n = 161$ ). **(m–o)** Correlations between the MFI of granzyme B in MAIT cells and the levels of plasma sST2 **(m)**, Gal-3 **(n)** and PICP **(o)** (data pairs  $n = 161$ ). Each symbol represents a single individual **(a–d, f–o)**. Heatmap colour intensity represents the correlation coefficient ( $r$ ) **(e)**. Statistical significance: ns  $P > 0.05$ ; \*  $P < 0.05$ ; \*\*  $P < 0.01$ ; \*\*\*  $P < 0.001$ ; \*\*\*\*  $P < 0.0001$ . Pearson correlation analysis was applied to panels **f–l**, while Spearman's correlation test was used for panels **m–o**.

negatively correlated with MAIT cell frequency but positively correlated with PICP and PIIINP levels. Moreover, elevated plasma LBP levels

exhibited positive correlations with the frequency of CD69<sup>+</sup> MAIT cells, as well as with PICP and PIIINP (Figure 6f–m).

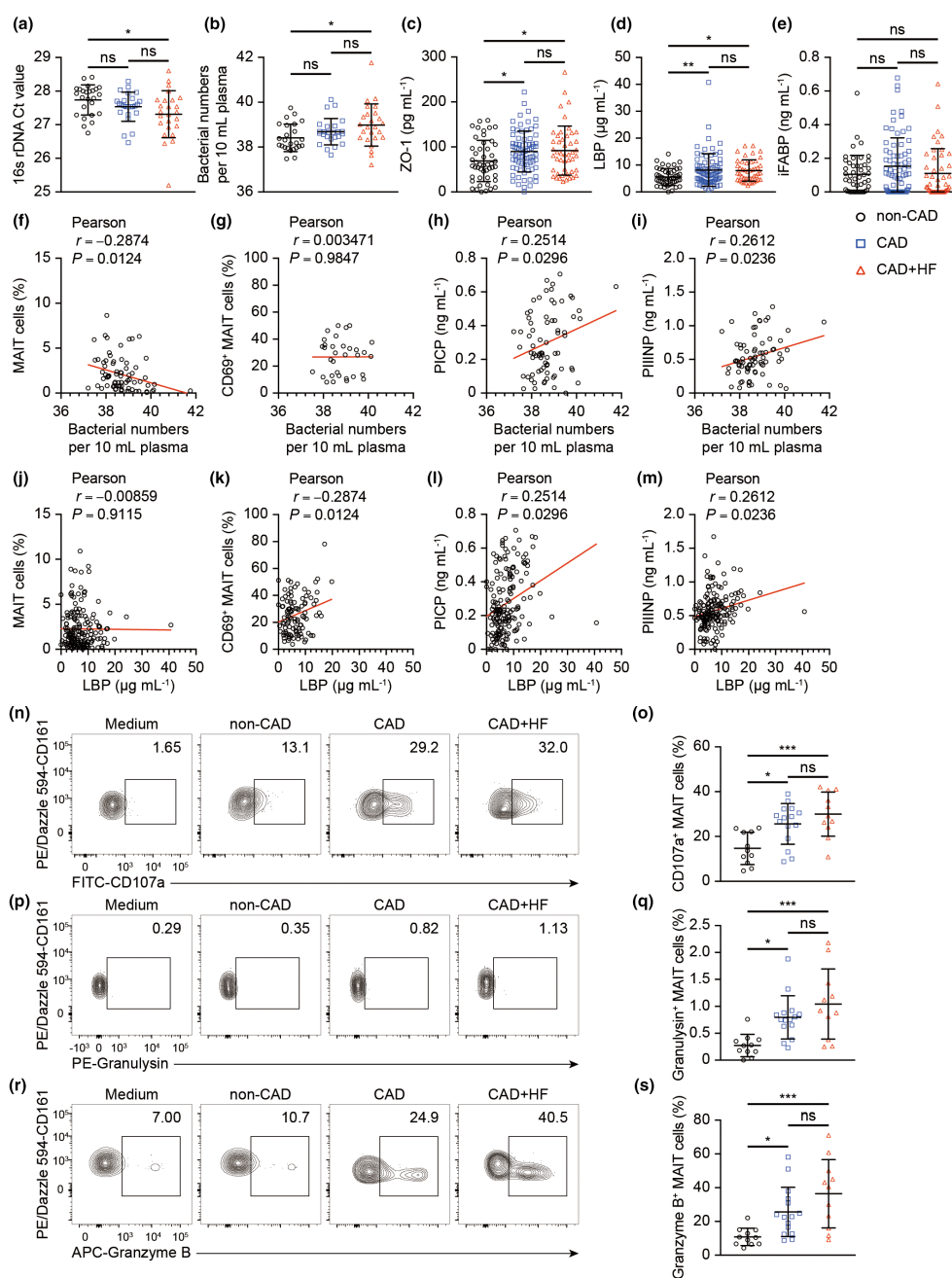


**Figure 6.** Gut barrier dysfunction and increased bacterial antigens may contribute to MAIT cell alterations. **(a, b)** Bacterial 16S rDNA detection by real-time PCR. **(a)** Cycle threshold (Ct) values and **(b)** bacterial counts per 10 mL of plasma, determined by absolute quantification using diluted *E. coli* as a standard curve, in samples from the non-CAD ( $n = 25$ ), CAD ( $n = 25$ ) and CAD + HF ( $n = 25$ ) groups. **(c–e)** ELISA quantification of plasma levels of tight junction protein ZO-1 **(c)**, LBP **(d)** and IFABP **(e)** in the non-CAD ( $n = 48$ ), CAD ( $n = 75$ ) and CAD + HF ( $n = 47$ ) groups. **(f–i)** Correlations between the bacterial number per 10 mL plasma and the frequency of MAIT cells **(f)** and CD69<sup>+</sup> MAIT cells **(g)**, as well as the levels of PICP **(h)** and PIINP **(i)** (data pairs,  $n = 75, 33, 75$  and  $75$ , respectively). **(j–m)** Correlations between plasma LBP concentration and MAIT cell frequency **(j)** and CD69<sup>+</sup> MAIT cells **(k)**, as well as the levels of PICP **(l)** and PIINP **(m)** (data pairs,  $n = 170, 103, 170$  and  $170$ , respectively). **(n–s)** Flow cytometry analysis showing the frequencies of CD107a<sup>+</sup> MAIT cells **(n, o)**, Granulysin<sup>+</sup> MAIT cells **(p, q)** and Granzyme B<sup>+</sup> MAIT cells **(r, s)** after *E. coli* stimulation in the non-CAD ( $n = 11$ ), CAD ( $n = 15$ ) and CAD + HF ( $n = 11$ ) groups or without stimulation (medium). Each symbol represents an individual sample **(a–m, o, q, s)**. Statistical significance: ns  $P > 0.05$ ; \*  $P < 0.05$ ; \*\*  $P < 0.01$ ; \*\*\*  $P < 0.001$ ; \*\*\*\*  $P < 0.0001$ . One-way ANOVA was conducted for comparisons among the three groups, followed by *post hoc* LSD analysis for pairwise comparisons. Pearson's correlation analysis was applied to panels f–m.

To further investigate the cytotoxic capacity of MAIT cells in response to bacterial antigens in the three groups, we stimulated them with bacterial antigens under physiological conditions. The Proteobacteria phylum has been reported to be highly stimulatory for MAIT cells, with *E. coli*, a bacterium with rich riboflavin metabolic pathways and a major species in the human gastrointestinal tract,<sup>33</sup> being a particularly potent stimulant. Therefore, we used *E. coli* as a microbial stimulus. During the degranulation of activated cytotoxic lymphocytes, the membrane of granules fuses with the cell membrane, leading to the exposure of CD107a molecules on the cell surface. Thus, the surface expression of CD107a is a sensitive marker for determining cytotoxic activity.<sup>42</sup> Upon stimulation with *E. coli*, the expression of CD107a, as well as the cytotoxic granules granzyme B, was markedly increased in MAIT cells from both CAD and CAD + HF patients compared with the non-CAD group (Figure 6n–s).

In conclusion, there is an increase in circulating bacterial levels in CAD patients, likely originating from intestinal barrier dysfunction. Bacterial antigens from the gut may act as a driving force behind the characteristic alterations of MAIT cells in patients with CAD and HF.

## DISCUSSION

Innate and adaptive immune responses play essential roles in the development of many cardiovascular diseases. Atherosclerosis, the primary cause of coronary artery disease, stroke and peripheral vascular disease, is widely recognised as a chronic inflammatory disease.<sup>43</sup> In recent years, significant progress has been made in understanding the roles of various immune cell types in the pathogenesis of cardiovascular diseases. For example, monocytes/macrophages within the innate immune system are closely linked to the formation of atherosclerotic plaques.<sup>44</sup> Th1 responses mediated by T helper cells in adaptive immune responses promote atherosclerosis, while CD8<sup>+</sup> T-cell-mediated myocardial injury contributes to cardiac ischaemia and adverse remodelling.<sup>9,45</sup> However, in-depth analyses of immune alterations across different stages of CAD and comprehensive assessments of specific immune alterations associated with CAD progression markers are still lacking.

In our study, we used multi-colour flow cytometry to evaluate the features of different

immune cell types in individuals with non-CAD, CAD and CAD with HF. Surprisingly, we found that MAIT cells, an unconventional T-cell subset, exhibited the most significant alterations among T-cell subsets in CAD patients relative to other immune cell types. MAIT cells have garnered increasing attention in the context of systemic inflammatory diseases over the past few years. They have been shown to be highly sensitive to inflammatory triggers in various chronic conditions with comorbid inflammation, including obesity, type 2 diabetes and autoimmune diseases.<sup>46–48</sup> However, research on MAIT cells in the cardiovascular field is still in its early stages. In 2018, Touch *et al.* reported a reduction in circulating MAIT cells in cardiometabolic diseases, but their study did not address how MAIT cells contribute to these diseases.<sup>19</sup> These previous studies, along with our observations, prompted us to investigate the role of MAIT cells in the progression of CAD and HF. We further discovered that in CAD patients, MAIT cells displayed enhanced activation and cytotoxicity, which significantly correlated with myocardial ischaemia, remodelling, and fibrosis. These correlations were assessed based on multiple indicators, including the degree of coronary artery stenosis, markers of myocardial injury and heart failure, as well as ultrasonic evaluations of cardiac structure and function.

Although it is well-established that inflammation plays a crucial role in the development and progression of CAD, the question of how this low-grade inflammation is initiated remains unclear, but it appears to be related to gut bacterial components.<sup>49</sup> The gut barrier functions to limit the escape of intestinal bacteria and toxic mediators from the gut, thereby preventing a systemic inflammatory response. Breakdown of the gut barrier leads to increased intestinal permeability, bacterial and endotoxin translocation into the systemic circulation, and activation of the immune-inflammatory system.<sup>50</sup> Multiple studies have shown that gut microbial dysbiosis is associated with CAD and cardiovascular risk. Elevated intestinal permeability has been observed following experimental myocardial infarction (MI) in rats.<sup>51</sup> Clinically, circulating lipopolysaccharide (LPS) levels have been found to be elevated in patients with MI when compared to healthy subjects.<sup>52</sup> Furthermore, Zhou *et al.* conducted a metagenomic analysis to characterise the systemic



bacteria in a cohort of CAD patients. They reported for the first time that the blood bacteria of CAD patients were positively correlated with systemic inflammation. Additionally, upon abrogation of gut bacterial translocation by antibiotic treatment, both systemic inflammation and cardiomyocyte injury were alleviated. This offers compelling evidence that the systemic inflammation in CAD could be driven by the translocation of intestinal microbiota into the systemic circulation.<sup>53</sup> While the microbiome in a specific human organs has been well-studied, few reports have investigated the microbiome and immunological processes as a whole. In our study, we also found that increased products of gut bacterial translocation were correlated with adverse cardiovascular events. More significantly, we discovered that bacteria could indeed trigger MAIT cell activation *in vitro*, thereby exhibiting a similar cytotoxic capacity to what we observed in CAD patients. This collectively suggests that gut barrier damage and increased bacterial antigens could serve as potential initiating factors for the characteristic changes in MAIT cells during the progression of CAD. Interestingly, we found a significant increase in granzyme B production by MAIT cells from CAD patients, especially those with HF, following the same amount of *E. coli* stimulation. We speculated that this could be because of either increased baseline cytotoxicity of MAIT cells from HF patients or MAIT cells being educated by bacterial antigens in HF patients, thus displaying a more sensitive or mature phenotype when given similar stimuli *in vitro*. Given the established role of granzyme B-mediated cell apoptosis in atherosclerosis,<sup>54</sup> our data suggest that MAIT cells may serve as a source of granzyme B, potentially influencing the progression and prognosis of CAD.

Given that these altered features of MAIT cells were more profound in CAD patients with HF complications, and myocardial fibrosis is the primary long-term pathological change in ischemic heart disease, contributing to the increased risk of HF and sudden cardiac death in CAD patients,<sup>55</sup> we explored the potential association between MAIT cells and myocardial fibrosis in our study. Although myocardial biopsy remains the definitive method for diagnosing myocardial fibrosis, numerous circulating biomarkers have been suggested for non-invasive evaluation of this condition.<sup>34</sup> In the heart, ST2-L and its ligand IL-33 mitigate cardiac injury and

adverse cardiac remodelling following stress by reducing fibrosis, hypertrophy and cell apoptosis. However, sST2 competes with ST2-L for IL-33, diminishing the beneficial effects of ST2-L/IL-33 signalling.<sup>35</sup> Hence, higher levels of sST2 are associated with more adverse cardiac remodelling and increased fibrosis. Gal-3 binds and activates fibroblasts, leading to the deposition of collagen into the extracellular matrix, thereby causing progressive cardiac fibrosis.<sup>36</sup> Furthermore, circulating levels of molecules related to collagen metabolism, such as PICP and PIIINP, have also been shown to be associated with histologically confirmed myocardial fibrosis.<sup>37,38</sup> In our study, all these fibrosis markers were significantly elevated in patients with CAD and HF, indicating the presence of myocardial fibrosis. Importantly, they exhibited significant correlations with the aforementioned changes in MAIT cell characteristics, suggesting that the alterations in MAIT cells may contribute to the progression of myocardial fibrosis.

In conclusion, our research revealed unique changes in MAIT cells during the progression of CAD, including decreased cell counts, increased activation, and enhanced cytotoxicity. These changes are closely associated with myocardial ischaemia, remodelling, and cardiac fibrosis, indicating that MAIT cells play a role in CAD progression by participating in the process of myocardial fibrosis. As such, MAIT cells could serve as a sensitive marker to identify individuals at high risk of CVD, thereby guiding targeted therapeutic strategies. However, our work does have several limitations. For instance, it remains uncertain whether these cells infiltrate and accumulate in the heart under CAD conditions. Therefore, more comprehensive immune cell profiling from coronary artery plaques and ischemic myocardial sites is necessary for identification and quantification. Second, while we observed that the altered features of MAIT cells were associated with CAD progression, it remains unclear whether MAIT cells were the cause or consequence of this process. This requires further investigation using animal models. Third, there are limitations to determining myocardial fibrosis using circulating markers. Although myocardial biopsies can be used for diagnosis, they may be difficult to implement. In contrast, obtaining the extracellular volume fraction (ECV) through cardiac magnetic resonance imaging (CMR) allows for both quantitative and localised diagnosis of myocardial fibrosis, making it

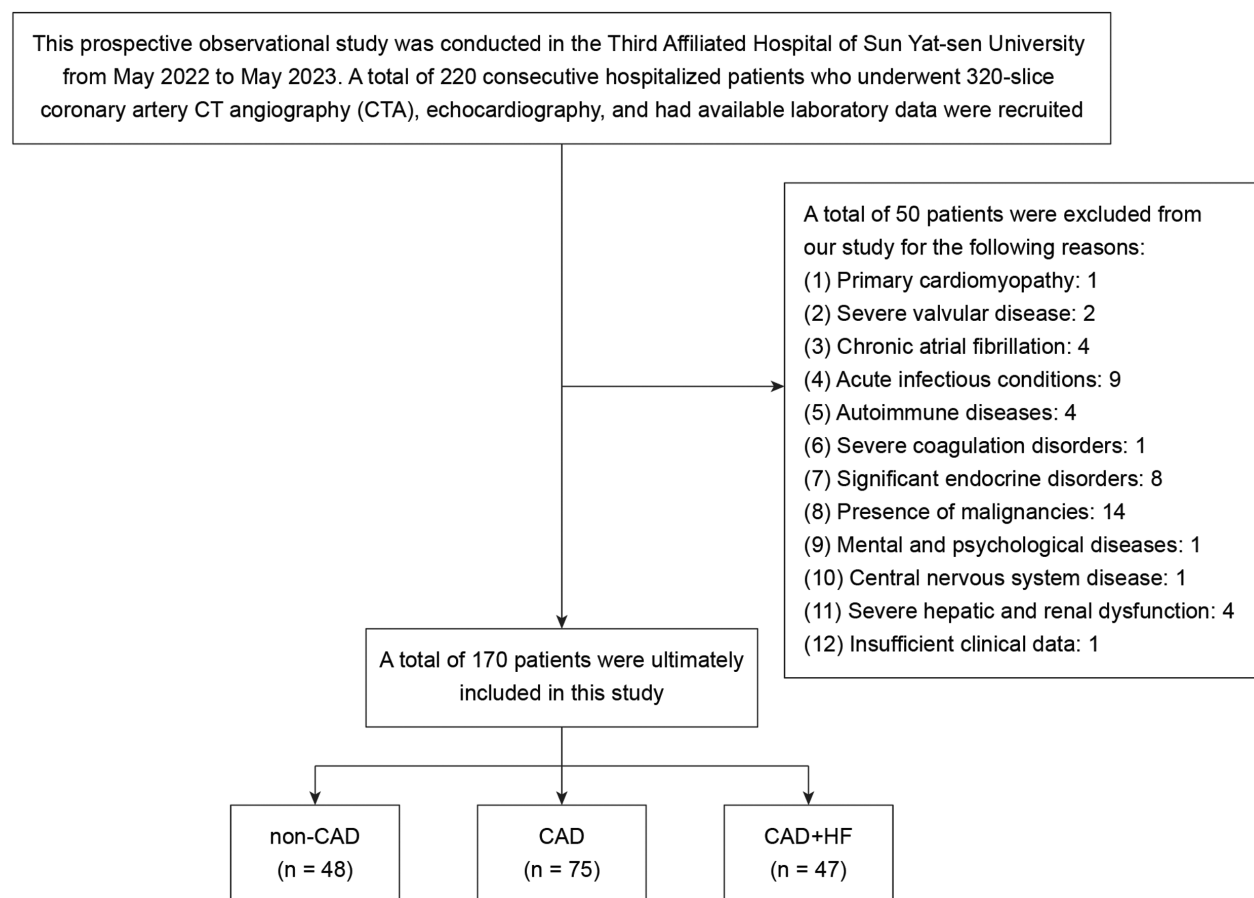


**Figure 7.** Flowchart depicting the study cohort. CAD, coronary artery disease; HF, heart failure.

a valuable tool for studying CAD populations. Finally, although we did observe elevated markers of intestinal barrier damage in the blood of CAD patients, which implies increased gut permeability and subsequent bacterial leakage, it should be noted that other sources, such as the oral cavity and skin, could also contribute to the presence of bacterial DNA in the bloodstream. Additionally, we could not distinguish whether the bacterial DNA in the blood originated from live bacteria or dead cell fragments. Further research using techniques such as fluorescence *in situ* hybridisation (FISH) and bacterial culture may help clarify this point.

## METHODS

### Study cohort

This single-center prospective study was conducted in the Department of Cardiovascular Medicine at the Third Affiliated Hospital of Sun Yat-sen University between May

2022 and May 2023. The design of subject inclusion, exclusion and grouping is depicted in Figure 7. A total of 220 consecutive hospitalised patients who underwent 320-slice coronary artery CT angiography (CTA), echocardiography, and with available laboratory data were recruited. Patients with a history of primary cardiomyopathy disease, severe valvular heart disease, chronic atrial fibrillation, acute infectious conditions, autoimmune diseases, severe coagulation disorders, significant endocrine disorders, malignancies, mental or psychological diseases, central nervous system disease, severe hepatic and renal dysfunction or insufficient clinical data were excluded. Finally, 170 patients were included in the analysis.

The diagnosis and grouping of CAD were based on patient symptoms and coronary artery CTA examinations, in accordance with the 2023 AHA/ACC/ACCP/ASPC/NLA/PCNA Guideline for the Management of Patients with Chronic Coronary Disease.<sup>56</sup> The diagnosis of concomitant HF was based on patient heart function classification, clinical presentations and laboratory examinations, in accordance with the 2022 AHA/ACC/HFSA Guideline for the Management of Heart Failure.<sup>57</sup> The study population was divided into three groups: (1) The non-CAD group consisted

of 48 patients who had no signs of CAD or HF and showed no evidence of cardiac structural damage. (2) The CAD group included 75 patients with CAD but without HF. (3) The CAD + HF group included 47 patients with CAD who also had HF. The research protocol was reviewed and approved by the Medical Ethics Committee of the Third Affiliated Hospital of Sun Yat-sen University [No. (2022) 02-193-01], in accordance with the ethical principles of the 1975 Helsinki Declaration. Written informed consent was obtained from all participants.

## Data collection

Demographic and clinical characteristics of all participants were collected, including age, sex, body mass index (BMI), blood pressure and history of hypertension. Fasting blood samples were collected from patients on the first morning of hospitalisation. The following haematological parameters were measured using an XN-Series Automated Hematology Analyzer (Sysmex, Kobe, Japan): absolute leukocyte count, absolute neutrophil count, absolute lymphocyte count, red cell distribution width standard deviation, haemoglobin, and absolute platelet count. Biochemical parameters, including total cholesterol, triglycerides, high-density lipoprotein cholesterol, low-density lipoprotein cholesterol, apoA1, apoB100, lipoprotein(a), homocysteine, serum creatinine, fasting blood glucose, lactate dehydrogenase, alkaline phosphatase and  $\gamma$ -glutamyl transferase, were determined using a Hitachi 7180 chemistry analyser (Hitachi High-Tech Corporation, Tokyo, Japan). Fibrinogen, D-dimer, serum ferritin and C-reactive protein (CRP) were measured using immunoassay methods.

## Assessment of systemic inflammatory status

Parameters to evaluate the immune system and inflammatory status of subjects included CRP, neutrophil-to-lymphocyte ratio (NLR), Systemic Immune-Inflammation Index (SII), Systemic Inflammation Response Index (SIRI) and Aggregate Index of Systemic Inflammation (AISI). The calculation methods for these indices were as previously reported,<sup>58</sup> and are briefly summarised as follows:

$$\text{NLR} = \text{Neutrophil count} / \text{Lymphocyte count}$$

$$\text{SII} = (\text{Platelet count} \times \text{Neutrophil count}) / \text{Lymphocyte count}$$

$$\text{SIRI} = \text{Neutrophil count} \times \text{Monocyte count} / \text{Lymphocyte count}$$

$$\text{AISI} = \text{Neutrophil count} \times \text{Monocyte count} \times \text{Platelet count} / \text{Lymphocyte count}.$$

## Plasma and PBMC preparation

Fresh venous blood samples (5 mL each) were collected from participants using vacuum blood collection tubes containing ethylenediaminetetraacetic acid (EDTA) anticoagulant. The blood samples were centrifuged at 3000 rpm for 10 min at 4°C, and the upper plasma layer was

carefully collected into Eppendorf tubes. These plasma samples were stored at -80°C in an ultra-low-temperature freezer until further use.

Peripheral blood mononuclear cells were isolated through density gradient centrifugation by layering the cellular fraction obtained after centrifugation onto Lymphoprep density gradient medium (STEMCELL Technologies, Vancouver, Canada). The PBMCs were resuspended in freezing culture medium containing dimethyl sulfoxide (DMSO) (Merck KGaA, Darmstadt, Germany) and fetal bovine serum (FBS) (ExCell Bio Group, Shanghai, China) and subsequently stored in liquid nitrogen until needed. The cryopreserved PBMCs were used for immunostaining, cell culture, and other experimental procedures.

## Flow cytometry analysis

Peripheral blood mononuclear cells were incubated with a blue LIVE/DEAD fixable dead cell stain (Thermo Fisher Scientific, Waltham, USA) for 15 min at room temperature to distinguish viable cells from non-viable ones. The cells were then gently washed and treated with a human Fc receptor blocking solution (BioLegend, San Diego, USA) for 15 min on ice to prevent non-specific antibody binding. Subsequently, PBMCs were surface-stained for 30 min on ice using the following anti-human monoclonal antibodies (mAbs): anti-CD107a (clone eBioH4A3), anti-CD14 (clone HCD14), anti-CD161 (clone HP-3G10), anti-CD19 (clone HIB19), anti-CD27 (clone LG.3A10), anti-CD3 (clone OKT3), anti-CD4 (clone OKT4), anti-CD69 (clone FN50), anti-CD8a (clone RPA-T8), anti-PD-1 (clone EH12.2H7), anti-TCR V $\alpha$ 24-J $\alpha$ 18 (clone 6B11), anti-TCR V $\alpha$ 7.2 (clone 3C10) and anti-TCR $\gamma\delta$  (clone B1) from BioLegend or Thermo Fisher Scientific.

For intracellular cytokine detection, PBMCs were stimulated with a 500 $\times$  diluted cell stimulation cocktail (plus protein transport inhibitors) containing 40.5  $\mu$ M PMA, 670  $\mu$ M ionomycin, 5.3 mM brefeldin A and 1 mM monensin (Thermo Fisher Scientific, Waltham, USA) for 6 h at 37°C in RPMI 1640 medium supplemented with 10% FBS. After surface staining, the cells were fixed and permeabilised using a fixation/permeabilisation kit (Becton, Dickinson and Company, Franklin Lakes, USA) according to the manufacturer's instructions, followed by staining with the following anti-human mAbs: anti-TNF- $\alpha$  (clone Mab11), anti-IFN- $\gamma$  (clone 4S.B3), anti-IL-17A (clone BL168), anti-Granulysin (clone DH2) and anti-Granzyme B (clone QA16A02) from BioLegend.

Data acquisition was performed using a BD LSRFortessa flow cytometer, and the data were analysed using the FlowJo v10.4 software (Becton, Dickinson and Company, Franklin Lakes, USA).

## Clinical evaluation of myocardial ischaemia and remodelling

The Gensini score was used to assess the burden of atherosclerotic plaques and the severity of stenosis in coronary arteries. This evaluation was conducted independently by two experienced cardiovascular experts

using a blinded approach, following the guidelines published by Gensini GG in 1983.<sup>59</sup> Detailed methods are presented in Supplementary figure 1.

Serum levels of cardiac troponin I (cTnI) were measured using either enzyme immunoassay (for screening) or enzyme immunochemiluminescence assay (for emergency situations) to evaluate the extent of myocardial ischaemia caused by atherosclerosis. Serum levels of N-terminal pro-B-type natriuretic peptide (NT-proBNP) were measured using enzyme immunoassay to assess the severity of heart failure and cardiac load.

Echocardiographic examination for cardiac structural and functional remodelling was performed on all participants using the Philips EPIQ 7C diagnostic ultrasound system, equipped with an S5-1 adult cardiac transducer (frequency 2.5–5.0 MHz) and the Philips QLab quantitative analysis workstation (Koninklijke Philips N.V., Amsterdam, the Netherlands). Three consecutive cardiac cycles of the apical four-chamber, three-chamber and two-chamber views were captured. Strain tracking echocardiography (STE) was used to delineate endocardial and epicardial borders in various regions of the heart, providing measurements of atrial and ventricular dimensions (left atrium, LA; right ventricle, RV; left ventricle, LV; right atrium, RA), interventricular septal (IVS) thickness and left ventricular posterior wall (LVPW) thickness. A long-axis view of the left ventricle was obtained in M-mode to assess endocardial motion, and parameters associated with mitral valve blood flow and motion were meticulously recorded using colour and tissue Doppler imaging. This comprehensive data set facilitated the assessment and computation of parameters related to both cardiac systolic (left ventricular ejection fraction, LVEF) and diastolic (E/e') function.

### Assessment of myocardial fibrosis biomarkers

Plasma levels of myocardial fibrosis biomarkers, including soluble suppression of tumorigenicity 2 protein (sST2), galectin-3 (Gal-3), the carboxy-terminal propeptide of type I procollagen (PICP) and the amino-terminal propeptide of type III procollagen (PIIINP), were quantified using ELISA methods according to the manufacturer's protocols, and the colour intensity was measured at 450 nm using the BioTek Synergy H1 Multimode Reader (Agilent Technologies, Santa Clara, USA). The sST2 and Gal-3 ELISA kits were purchased from Meimian (Jiangsu Meimian Industrial, Yancheng, China), the PIIINP ELISA kit from Elabscience (Elabscience Biotechnology, Wuhan, China) and the PICP ELISA kit from CUSABIO (CUSABIO Technology, Wuhan, China).

### 16S rDNA extraction and quantification

Total DNA was extracted from plasma samples using the ZymoBIOMICS DNA Miniprep kit (Zymo Research Corporation, Irvine, USA). All procedural steps were conducted within a sterile biological safety cabinet to minimise the risk of contamination. Bacterial DNA quantification was performed via real-time PCR using the 16S rDNA primer pair 27F: 5'-AGAGTTTGATCMTGGCTCAG-3'

and 1492R: 5'-TACGGYTACCTTGTTACGACTT-3'. Real-time PCR analysis was conducted on the LightCycler 480 Instrument II (Roche Diagnostics, Indianapolis, USA). Ct values were obtained for each reaction and used for data analysis. A standard curve generated using *E. coli* genomic DNA was employed to determine the absolute bacterial quantities measured by real-time PCR.

### Measurement of intestinal barrier function markers

Plasma levels of intestinal barrier dysfunction markers, including tight junction protein 1 (ZO-1), lipopolysaccharide-binding protein (LBP) and intestinal fatty acid-binding protein (IFABP), were quantified using ELISA methods as previously described. The ELISA kits for these markers were purchased from CUSABIO (CUSABIO Technology, Wuhan, China).

### Bacterial stimulation experiments

To assess the cytotoxicity of human MAIT cells in response to bacterial stimulation, the following protocol was used: Initially, *E. coli* (strain DH10B) was revived in 5 mL Luria-Bertani (LB) medium and cultured overnight in a shaking incubator at 37°C with a speed of 200 rpm. Subsequently, the bacterial suspension was diluted until an optical density (OD) of 1.0 at 600 nm (approximately 10<sup>8</sup> bacteria per mL) was achieved, as measured using a NanoDrop One Microvolume UV-Vis Spectrophotometer (Thermo Fisher Scientific, Waltham, USA). A 1-mL aliquot of the diluted bacterial suspension was centrifuged at 5000 × g for 3 min at 4°C. After discarding the supernatant, the bacterial pellet was fixed with 2% paraformaldehyde (PFA). Following fixation, the *E. coli* was resuspended in 1 mL of RPMI 1640 culture medium. A 10 µL volume of the prepared bacterial suspension was added to PBMCs resuspended in RPMI 1640 culture medium containing 10% FBS. The mixture was incubated at 37°C in a 5% CO<sub>2</sub> incubator for a total of 12 h, with Brefeldin A (BioLegend, San Diego, USA) added during the final 4 h of incubation. After incubation, the cells were collected and analysed by flow cytometry using the methods described previously.

### Statistical analysis

Statistical analyses were performed using the SPSS software version 22.0 or GraphPad Prism version 10. Categorical variables were expressed as percentages, while continuous variables with a normal distribution were presented as mean ± standard deviation (SD), and those with a non-normal distribution as median with interquartile range (IQR). Continuous variables were compared using analysis of variance (ANOVA), and categorical variables were compared using the Pearson Chi-squared test. Receiver operating characteristic (ROC) curves were generated to evaluate the predictive values of immune cell abundance for differentiating between CAD and CAD+HF patients. Pearson or Spearman correlation analyses were used to investigate the relationships between MAIT cell characteristics and indicators of atherosclerosis severity and

HF, the associations between MAIT cells and myocardial fibrosis markers, and the links between intestinal bacterial leakage and MAIT cell alterations. Unless otherwise specified, a two-tailed *P*-value < 0.05 was considered statistically significant.

## ETHICS APPROVAL

This study and the associated experimental procedures were approved by the Ethics Committee of the Third Affiliated Hospital of Sun Yat-sen University [Approval No. (2022) 02–193-01]. Informed consent was obtained from all participants following a process reviewed by the same Ethics Committee. The study was conducted in accordance with the ethical standards outlined in the Declaration of Helsinki.

## PATIENT CONSENT

Participants provided written informed consent for the use of their clinical data and radiological examination records, including consent for publication.

## ACKNOWLEDGMENTS

We extend our gratitude to all the patients who participated in this study. Funding for this research was provided by the National Natural Science Foundation of China (82200384, 32470950, 82300923 and 82300991), the Guangdong Basic and Applied Basic Research Foundation (2022A1515220129, 2022A1515110173, 2023A1515010526, 2023A1515012417 and 2024A1515011892), the Science and Technology Project in Guangzhou (2023A04J1081, 2024A03J0175, 2024A04J4783, 2025A03J3827 and 2025A03J3824), the Guangdong Provincial Medical Research Fund (A2022076 and A2022361), the Fostering of Special Funding Projects of the National Natural Science Foundation of China in the Third Affiliated Hospital of SYSU (2021GZRPYQN11) and the Third Affiliated Hospital of Sun Yat-sen University Clinical Medical Research Special Fund “Sailing Program” (QJHJ202201).

## AUTHOR CONTRIBUTIONS

**Jiafu Wang:** Data curation; formal analysis; investigation; methodology; writing – original draft. **Song Li:** Data curation; formal analysis; investigation; methodology; writing – original draft. **Xianling Zhou:** Data curation; formal analysis; investigation; methodology; writing – original draft. **Hongxing Wu:** Investigation. **Xiaolan Ouyang:** Investigation. **Zhuoshan Huang:** Investigation. **Long Peng:** Funding acquisition; investigation. **Qian Chen:** Investigation. **Yuman Wu:** Investigation. **Zhitong Li:** Investigation. **Ziyi Peng:** Investigation. **Yi Yang:** Funding acquisition; investigation. **Yan Lu:** Conceptualization; funding acquisition; investigation; methodology; project administration; supervision; validation; writing – original draft; writing – review and editing. **Xixiang Tang:** Conceptualization; funding acquisition; investigation; methodology; project administration; resources; supervision;

writing – original draft; writing – review and editing. **Yue Li:** Conceptualization; funding acquisition; investigation; methodology; project administration; supervision; writing – original draft; writing – review and editing. **Suhua Li:** Conceptualization; funding acquisition; investigation; methodology; project administration; resources; supervision; writing – original draft; writing – review and editing.

## CONFLICT OF INTEREST

The authors declare no conflict of interest.

## DATA AVAILABILITY STATEMENT

The data supporting the findings of this study are available upon reasonable request from the corresponding authors.

## REFERENCES

1. Dai H, Much AA, Maor E *et al.* Global, regional, and national burden of ischaemic heart disease and its attributable risk factors, 1990–2017: Results from the global burden of disease study 2017. *Eur Heart J Qual Care Clin Outcomes* 2022; **8**: 50–60.
2. Talman V, Ruskoaho H. Cardiac fibrosis in myocardial infarction-from repair and remodeling to regeneration. *Cell Tissue Res* 2016; **365**: 563–581.
3. Khatibzadeh S, Farzadfar F, Oliver J, Ezzati M, Moran A. Worldwide risk factors for heart failure: A systematic review and pooled analysis. *Int J Cardiol* 2013; **168**: 1186–1194.
4. Ajoolabady A, Pratico D, Lin L *et al.* Inflammation in atherosclerosis: Pathophysiology and mechanisms. *Cell Death Dis* 2024; **15**: 817.
5. Henein MY, Vancheri S, Longo G, Vancheri F. The role of inflammation in cardiovascular disease. *Int J Mol Sci* 2022; **23**: 12906.
6. Dib L, Koneva LA, Edsfeldt A *et al.* Lipid-associated macrophages transition to an inflammatory state in human atherosclerosis increasing the risk of cerebrovascular complications. *Nat Cardiovasc Res* 2023; **2**: 656–672.
7. Koelwyn GJ, Corr EM, Erbay E, Moore KJ. Regulation of macrophage immunometabolism in atherosclerosis. *Nat Immunol* 2018; **19**: 526–537.
8. Jebari-Benslaiman S, Galicia-Garcia U, Larrea-Sebal A *et al.* Pathophysiology of atherosclerosis. *Int J Mol Sci* 2022; **23**: 3346.
9. Santos-Zas I, Lemarie J, Zlatanova I *et al.* Cytotoxic CD8<sup>+</sup> T cells promote granzyme B-dependent adverse post-ischemic cardiac remodeling. *Nat Commun* 2021; **12**: 1483.
10. Ali M, Girgis S, Hassan A, Rudick S, Becker RC. Inflammation and coronary artery disease: From pathophysiology to canakinumab anti-inflammatory thrombosis outcomes study (CANTOS). *Coron Artery Dis* 2018; **29**: 429–437.
11. Niu Y, Bai N, Ma Y, Zhong PY, Shang YS, Wang ZL. Efficacy of intravascular imaging-guided drug-eluting stent implantation: A systematic review and meta-analysis of randomized clinical trials. *BMC Cardiovasc Disord* 2022; **22**: 327.



12. Ridker PM, MacFadyen JG, Everett BM et al. Relationship of C-reactive protein reduction to cardiovascular event reduction following treatment with canakinumab: A secondary analysis from the CANTOS randomised controlled trial. *Lancet* 2018; **391**: 319–328.
13. Diamantis E, Kyriakos G, Quiles-Sanchez LV, Farmaki P, Troupis T. The anti-inflammatory effects of statins on coronary artery disease: An updated review of the literature. *Curr Cardiol Rev* 2017; **13**: 209–216.
14. Oesterle A, Laufs U, Liao JK. Pleiotropic effects of statins on the cardiovascular system. *Circ Res* 2017; **120**: 229–243.
15. Dias J, Leeansyah E, Sandberg JK. Multiple layers of heterogeneity and subset diversity in human MAIT cell responses to distinct microorganisms and to innate cytokines. *Proc Natl Acad Sci USA* 2017; **114**: E5434–E5443.
16. Kurioka A, Ussher JE, Cosgrove C et al. MAIT cells are licensed through granzyme exchange to kill bacterially sensitized targets. *Mucosal Immunol* 2015; **8**: 429–440.
17. Hwang Y, Yu HT, Kim DH et al. Expansion of CD8<sup>+</sup> T cells lacking the IL-6 receptor alpha chain in patients with coronary artery diseases (CAD). *Atherosclerosis* 2016; **249**: 44–51.
18. Li Y, Yang Y, Wang J et al. *Bacteroides ovatus*-mediated CD27<sup>+</sup> MAIT cell activation is associated with obesity-related T2D progression. *Cell Mol Immunol* 2022; **19**: 791–804.
19. Touch S, Assmann KE, Aron-Wisnewsky J et al. Mucosal-associated invariant T (MAIT) cells are depleted and prone to apoptosis in cardiometabolic disorders. *FASEB J* 2018; **32**: 4625–5210.
20. Borger JG, Lau M, Hibbs ML. The influence of innate lymphoid cells and unconventional T cells in chronic inflammatory lung disease. *Front Immunol* 2019; **10**: 1597.
21. Hegde P, Weiss E, Paradis V et al. Mucosal-associated invariant T cells are a profibrogenic immune cell population in the liver. *Nat Commun* 2018; **9**: 2146.
22. Law BMP, Wilkinson R, Wang X et al. Human tissue-resident mucosal-associated invariant T (MAIT) cells in renal fibrosis and ckd. *J Am Soc Nephrol* 2019; **30**: 1322–1335.
23. Gulden E, Palm N, Herold KC. MAIT cells: A link between gut integrity and type 1 diabetes. *Cell Metab* 2017; **26**: 813–815.
24. Kazemian N, Mahmoudi M, Halperin F, Wu JC, Pakpour S. Gut microbiota and cardiovascular disease: Opportunities and challenges. *Microbiome* 2020; **8**: 36.
25. Zhang B, Wang X, Xia R, Li C. Gut microbiota in coronary artery disease: A friend or foe? *Biosci Rep* 2020; **40**: BSR20200454.
26. Meng LB, Yu ZM, Guo P et al. Neutrophils and neutrophil-lymphocyte ratio: Inflammatory markers associated with intimal-media thickness of atherosclerosis. *Thromb Res* 2018; **170**: 45–52.
27. Dziedzic EA, Gasior JS, Tuzimek A et al. Investigation of the associations of novel inflammatory biomarkers-systemic inflammatory index (SII) and systemic inflammatory response index (SIRI)-with the severity of coronary artery disease and acute coronary syndrome occurrence. *Int J Mol Sci* 2022; **23**: 9553.
28. Xiu J, Lin X, Chen Q et al. The aggregate index of systemic inflammation (AISI): A novel predictor for hypertension. *Front Cardiovasc Med* 2023; **10**: 1163900.
29. Milo-Cotter O, Teerlink JR, Metra M et al. Low lymphocyte ratio as a novel prognostic factor in acute heart failure: Results from the pre-RELAX-AHF study. *Cardiology* 2010; **117**: 190–196.
30. Kurioka A, Klennerman P. Aging unconventionally: Gammadelta T cells, iNKT cells, and MAIT cells in aging. *Semin Immunol* 2023; **69**: 101816.
31. Cibrian D, Sanchez-Madrid F. CD69: From activation marker to metabolic gatekeeper. *Eur J Immunol* 2017; **47**: 946–953.
32. Starzer AM, Berghoff AS. New emerging targets in cancer immunotherapy: CD27 (TNFRSF7). *ESMO Open* 2020; **4**: e000629.
33. Tastan C, Karhan E, Zhou W et al. Tuning of human MAIT cell activation by commensal bacteria species and MR1-dependent T-cell presentation. *Mucosal Immunol* 2018; **11**: 1591–1605.
34. Lopez B, Gonzalez A, Ravassa S et al. Circulating biomarkers of myocardial fibrosis: The need for a reappraisal. *J Am Coll Cardiol* 2015; **65**: 2449–2456.
35. Sanada S, Hakuno D, Higgins LJ, Schreiter ER, McKenzie AN, Lee RT. IL-33 and ST2 comprise a critical biomechanically induced and cardioprotective signaling system. *J Clin Invest* 2007; **117**: 1538–1549.
36. Leone M, Iacoviello M. The predictive value of plasma biomarkers in discharged heart failure patients: Role of galectin-3. *Minerva Cardioangiol* 2016; **64**: 181–194.
37. Querejeta R, Lopez B, Gonzalez A et al. Increased collagen type I synthesis in patients with heart failure of hypertensive origin: Relation to myocardial fibrosis. *Circulation* 2004; **110**: 1263–1268.
38. Izawa H, Murohara T, Nagata K et al. Mineralocorticoid receptor antagonism ameliorates left ventricular diastolic dysfunction and myocardial fibrosis in mildly symptomatic patients with idiopathic dilated cardiomyopathy: A pilot study. *Circulation* 2005; **112**: 2940–2945.
39. Kuziel GA, Rakoff-Nahoum S. The gut microbiome. *Curr Biol* 2022; **32**: R257–R264.
40. Tang TWH, Chen HC, Chen CY et al. Loss of gut microbiota alters immune system composition and cripples postinfarction cardiac repair. *Circulation* 2019; **139**: 647–659.
41. Timmermans K, Sir O, Kox M et al. Circulating iFABP levels as a marker of intestinal damage in trauma patients. *Shock* 2015; **43**: 117–120.
42. Aktas E, Kucuksezer UC, Bilgic S, Erten G, Deniz G. Relationship between CD107a expression and cytotoxic activity. *Cell Immunol* 2009; **254**: 149–154.
43. Fernandez-Ruiz I. Immune system and cardiovascular disease. *Nat Rev Cardiol* 2016; **13**: 503.
44. Guo Z, Wang L, Liu H, Xie Y. Innate immune memory in monocytes and macrophages: The potential therapeutic strategies for atherosclerosis. *Cells* 2022; **11**: 4072.
45. Chen J, Xiang X, Nie L et al. The emerging role of Th1 cells in atherosclerosis and its implications for therapy. *Front Immunol* 2022; **13**: 1079668.
46. Hinks TS. Mucosal-associated invariant T cells in autoimmunity, immune-mediated diseases and airways disease. *Immunology* 2016; **148**: 1–12.

47. Magalhaes I, Pingris K, Poitou C et al. Mucosal-associated invariant T cell alterations in obese and type 2 diabetic patients. *J Clin Invest* 2015; **125**: 1752–1762.
48. Toubal A, Kiaf B, Beaudoin L et al. Mucosal-associated invariant T cells promote inflammation and intestinal dysbiosis leading to metabolic dysfunction during obesity. *Nat Commun* 2020; **11**: 3755.
49. Katsimichas T, Theofilis P, Tsioufis K, Tousoulis D. Gut microbiota and coronary artery disease: Current therapeutic perspectives. *Metabolites* 2023; **13**: 256.
50. Ma Y, Yang X, Villalba N et al. Circulating lymphocyte trafficking to the bone marrow contributes to lymphopenia in myocardial infarction. *Am J Physiol Heart Circ Physiol* 2022; **322**: H622–H635.
51. Levy WC, Mozaffarian D, Linker DT et al. The seattle heart failure model: Prediction of survival in heart failure. *Circulation* 2006; **113**: 1424–1433.
52. Anzulovic-Mirosevic D, Barzon L, Castagliuolo I et al. LPS in patients with left ventricular dysfunction of ischemic and non-ischemic origin. *Cardiovasc Hematol Disord Drug Targets* 2011; **11**: 74–78.
53. Zhou X, Li J, Guo J et al. Gut-dependent microbial translocation induces inflammation and cardiovascular events after ST-elevation myocardial infarction. *Microbiome* 2018; **6**: 66.
54. Kyaw T, Winship A, Tay C et al. Cytotoxic and proinflammatory CD8<sup>+</sup> T lymphocytes promote development of vulnerable atherosclerotic plaques in apoE-deficient mice. *Circulation* 2013; **127**: 1028–1039.
55. Thiene G. Ischaemic myocardial fibrosis is the villain of sudden coronary death. *Eur Heart J* 2022; **43**: 4931–4932.
56. Virani SS, Newby LK, Arnold SV et al. 2023 AHA/ACC/ACCP/ASPC/NLA/PCNA guideline for the management of patients with chronic coronary disease: A report of the american heart association/american college of cardiology joint committee on clinical practice guidelines. *Circulation* 2023; **148**: e9–e119.
57. Heidenreich PA, Bozkurt B, Aguilar D et al. 2022 AHA/ACC/HFSA guideline for the management of heart failure: A report of the american college of cardiology/american heart association joint committee on clinical practice guidelines. *J Am Coll Cardiol* 2022; **79**: e263–e421.
58. Li J, He D, Yu J et al. Dynamic status of SII and SIRI alters the risk of cardiovascular diseases: Evidence from Kailuan cohort study. *J Inflamm Res* 2022; **15**: 5945–5957.
59. Gensini GG. A more meaningful scoring system for determining the severity of coronary heart disease. *Am J Cardiol* 1983; **51**: 606.

## Supporting Information

Additional supporting information may be found online in the Supporting Information section at the end of the article.



This is an open access article under the terms of the [Creative Commons Attribution-NonCommercial](https://creativecommons.org/licenses/by-nc/4.0/) License, which permits use, distribution and reproduction in any medium, provided the original work is properly cited and is not used for commercial purposes.